

# FIRST NUMERICAL WAKEFIELD STUDIES OF NEW IN-VACUUM CRYOGENIC AND APPLE II UNDULATORS FOR BESSY II

M. Huck\*, J. Bahrtdt, A. Meseck

Helmholtz-Zentrum Berlin für Materialien und Energie (HZB), Berlin, Germany

## Abstract

While the new in-vacuum cryogenic undulator is in its last commissioning stages, a worldwide new in-vacuum APPLE II undulator is being designed and constructed for BESSY II storage ring. Besides the challenging mechanical design of these small-gap and short-period undulators, challenges arise due to interaction with the electron beam. Therefore, detailed studies of this interaction is required to minimize the adverse effects on beam dynamics and the device itself. For this purpose, the wakefield effects have been computed numerically for critical parts of these devices i.e. the RF-shields, flexible tapers and taper sections. A brief overview of simulation results and discussions are presented in this paper.

## INTRODUCTION

The first cryogenic permanent magnet undulator (CPMU17) has been installed in 2018 at BESSY II, and since then this device has served as a light source for beamline commissioning [1] and recently, for first user experiments. Beam-based studies to investigate the impedance of the device using orbit-bump, tune-shift and grow-damp techniques can be found in [2,3]. Furthermore, a worldwide new in-vacuum APPLE II undulator (IVUE32) with 32 mm period length is under construction [4,5]. The results of these various studies are required for designing new in-vacuum devices in future.

## CPMU17 STRUCTURE AND SIMULATION

Figures 1 and 2 show the schematics of CPMU17 vacuum components and CST models. Standard RF-shields made of a 50  $\mu\text{m}$  Copper layer coated on a 50  $\mu\text{m}$  thick Nickel foil screens the discontinuities of the magnets. The thickness of the Copper coating is larger than its skin depth at the frequency range of interest. The Nickel side is attracted by magnetic forces whereas the Copper side faces the electron beam. A taper made of Copper-Beryllium alloy connects the magnet part to the flexible taper mechanics (taper section). One end of the taper has a fixed height of  $g_f = 11$  mm and the other end has a height equal to the magnetic gap. Down- and upstream of the ID, there are transition bellows with cross section varying from elliptical to octagonal form. The magnet-shield-length and -width amounts to  $LM = 1517$  mm and  $w = 46$  mm, respectively, and the taper is  $LT = 119.4$  mm long. The small discontinuous regions inside the taper section (shown in Fig. 2c as d) changes its length in operational cooled state from  $d \sim 3.13$  mm at gap of  $g = 22$  mm to  $d \sim 3.0$  mm at  $g = 11$  mm. There is also

a rectangle-ellipse transition-part between the taper section and the entrance and exit flanges of the vessel.

The simulations for both IVUs in this study were carried out using the wakefield solver of the CST particle-studio tool [6] with a single-bunch of rms length of  $\sigma_b = 8.4$  mm (28 ps), and  $8 \times 10^{-9}$  C (10 mA) charge, which are the beam parameters in our measurements in [2]. The material of CST model was vacuum, surrounded by a perfect electric-conductor (PEC) material. An extra end section with length of  $Le = 100$  mm is used, in the longitudinal direction, extending to infinity with open boundary condition. The result of simulations are shown in Fig. 3.

The **longitudinal impedance  $Z_z(\nu)$  and wake potential  $W(z)$**  in Figs. 3a and 3b has been simulated using 140 cell per wavelength,  $dz = 0.08$  mm mesh size in  $z$  plane at taper, 0.17 mm in other planes, and 422 million mesh cells. It can be seen that  $Z_z$  increases smoothly at low frequencies ( $\nu < 8$  GHz) presenting the broadband part of the impedance. At high frequencies, the longitudinal impedance exhibits many resonant peaks at different frequencies depending on the gap size due to cavity like form of the structure. The minimum impedance is, as expected, at  $g = 11$  mm, where the taper is flat. The largest impedance  $\sim 43 \Omega$  occurs at gap of 22 mm, where the taper is steepest, and the structure has a cavity form. As comparisons, the impedance of the transition bellow can be mentioned, with a sharp peak of 1.4 k $\Omega$  at 4.2 GHz. Furthermore, in [7], the  $\text{Im}(Z_z)$  of mode 396 was measured amounting to 373 k $\Omega$ .

The small bump at the wake potential could be sign of numerical dispersion affecting the results in terms of loss factor and it can be resolved by using more mesh cells.

Figure 3c shows the  $Z_z(\nu)$  for a *shorter bunch* with  $\sigma_b = 16$  ps and 0.3 mA (0.24 nC) bunch current (low alpha mode at BESSY II). The spectrum extends to 20.5 GHz, and the maximum  $Z_z(\nu)$  amounts to 475  $\Omega$ .

For calculating the **transverse dipolar impedance  $Z_y(\nu)$** , the beam was located at  $y_b = 0.2$  mm, and the test beam at the center of ID. For the **quadrupolar impedance**, the location of the source and test beams was flipped. This simulation approach has been described in [8–10] and was also used in [11]. Since the dipolar and vertical impedance is

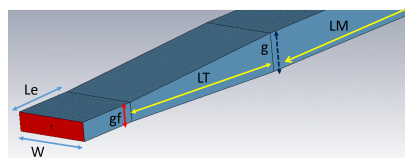


Figure 1: Downstream part of CST model for magnet foils and tapers, symmetric with the upstream part.

\* maryam.huck@helmholtz-berlin.de

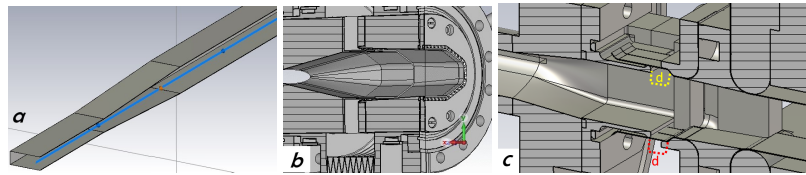


Figure 2: CST model of PEC foils and taper, cut in middle (a), CAD model of transition bellow (b) and taper section (c).

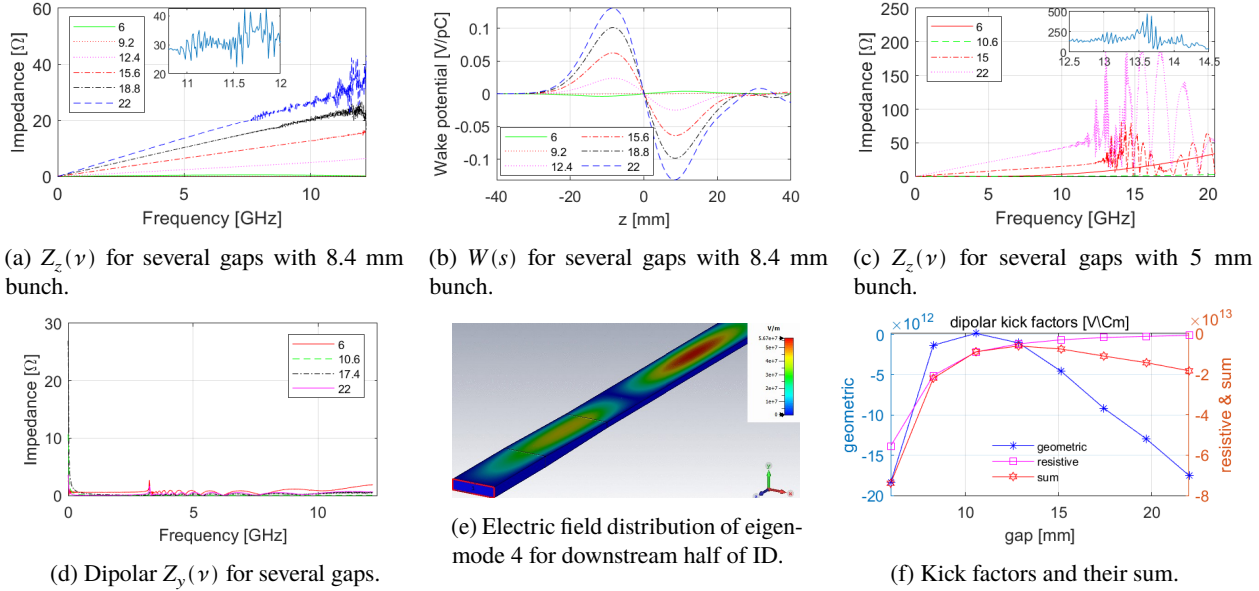


Figure 3: Simulation results for CPMU17.

larger and more relevant than the quadrupolar and horizontal one, we present here only the spectra for vertical-dipolar impedances. The number of cells per wavelength used for these calculations ( $\sim 20$ ) and total mesh numbers are less than that used for the longitudinal direction. An example of  $Z_y$  spectra for 4 ID gaps is shown in Fig. 3d; It can be seen, that the spectrum has a peak of  $Z_y(\nu) = 3.4 \Omega$  at  $\nu = 3.3$  GHz (at gap of 6 mm), corresponding to mode 4, derived by eigenmode solver. The electric field distribution of this mode is shown in Fig. 3e for the half downstream of ID (symmetric with upstream). The field has a maximum of 5.7 V/m and is distributed on top and bottom of the RF shields and taper. At low frequencies ( $<200$  MHz), the vertical impedance increases fast, and reaches to the amount of  $\sim 20 \Omega$  at zero frequency.

A vertical offset of the test beam with respect to the source beam ( $dy$ ) results in **transverse kick factors**, defined as convolution of transverse wake potential with normed charge distribution function over  $z$  divided by offset  $dy$  [2, 6, 12]. The dipolar "geometric" (shields and tapers without resistance), and resistive-wall kick-factors versus ID-gap, and their sum is shown in Fig. 3f. The maximum of sum kick-factor amounts to  $\sim -8 \times 10^{13}$  V/Cm at gap of 6 mm. In addition, the contribution of the taper section (Fig. 2c) is almost equal for all gaps amounting to  $\approx 1.5 \times 10^{14}$  V/Cm. For comparison, the kick factor arising from each bellow, under the same simulation condition, was  $1.9 \times 10^{14}$  V/Cm.

The results are to some extent in agreement with the experimental results [2], but an exact comparison needs further investigation in more details. The resistive-wall impedance of CPMU17 should also be calculated again considering anomalous skin depth effects of the thin Copper shields at cryogenic temperature.

## IVUE32 STRUCTURE AND SIMULATION

The structure of the IVUE32 has been described in detail in [4,5]. Here, we consider only the immediate parts seen by electrons i.e. the RF shields and tapers. IVUE32 consists of 4 magnet rows, with horizontal separation of  $\sim 0.8$  mm. Each magnet row is covered with an individual foil which is canted at the slit close to the beam axis. The rows are movable independently in longitudinal direction (for the polarization adjustment), and individual RF shields follow the same motion pattern. Differently, the taper foils are

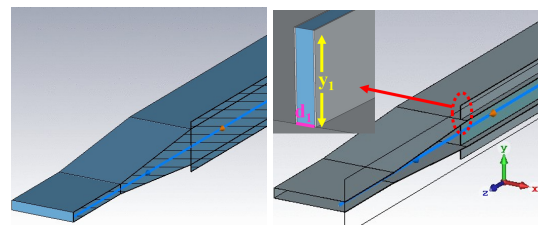


Figure 4: Two CST models for IVUE32 (at downstream part), each one cut at the horizontal center of the structure.

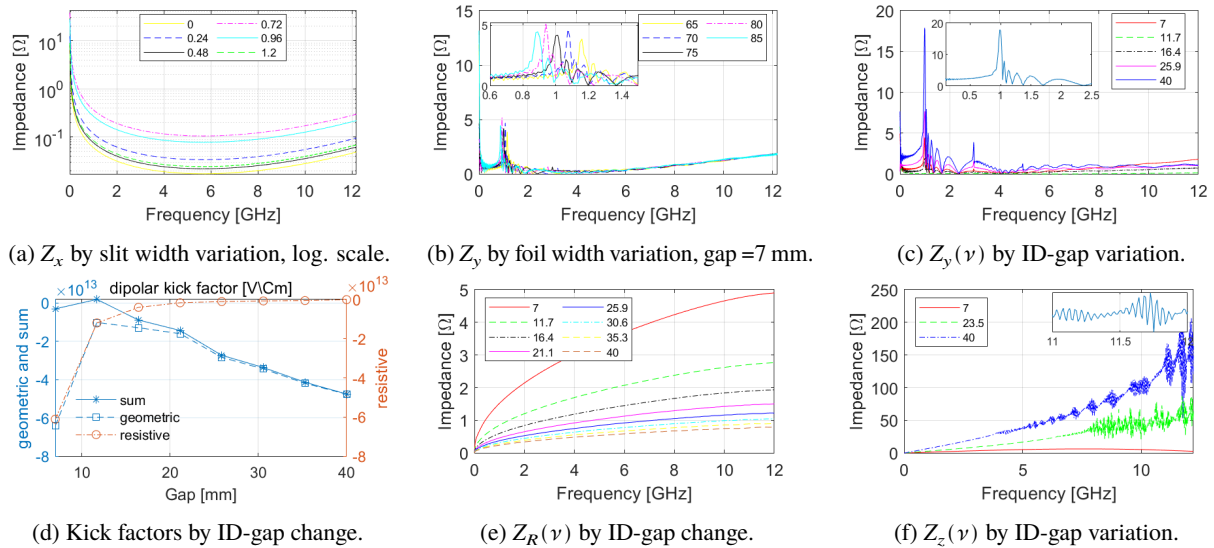


Figure 5: IVUE32 impedance spectra and kick factors by variation of different parameters.

made as a single piece. The magnetic length is 2664 mm, foil width 75 mm, and taper length 150 mm. The material properties of foils will be similar to those of CPMU17.

**2 variants** of a CST model for such structure is shown in Fig. 4. In first model (left), the structure is made of vacuum and the background is PEC. In second model, the background is vacuum and RF shields and tapers are PEC with side walls only at the end sections or along the entire ID. In this paper the results of the first variant are presented except for Fig. 5f. An increased number of meshes was used across the canted slit and along tapers.

**Firstly**, simulations were done by sweeps over slit width  $d_1$  (Fig. 5a) and height  $y_1$  and foil width  $w$  (Fig. 5b) at gap of 7 mm. The results shows that, except for minor variation the impedances in 3 planes do not respond significantly to changes in these parameters

**Secondly**, with  $d_1 = 0.8$  mm,  $y_1 = 3$  mm and  $w = 75$  mm, the impedance spectra in vertical plane  $Z_y(\nu)$  (Fig. 5c), longitudinal plane  $Z_c(\nu)$  (Fig. 5f), and dipolar vertical kick factors (Fig. 5d) were simulated. Resonant peaks can be observed at longitudinal spectra, especially at larger gaps due to cavity-like form. However, by increasing the mesh numbers, these peaks get less sharper. In vertical plane resonances occur at about 1, 3 and 5 GHz.

To simulate the **resistive impedance**  $Z_R(\nu)$ , two parallel Copper plates with a length equal to  $LM$  have been used. As expected, the magnitude of the resistive impedance and the resistive kick factor were decreasing by increasing the gap, and  $Z_R(\nu)$  increases with the frequency (Fig. 5e). In spite of high conductivity of Copper foil, the resistive wall impedance of the long undulator with narrow gaps contributes considerably into the kick factor (Fig. 5d), comparable to the geometric impedance.

### Remarks and Discussion

While the preliminary simulations suggested the results shown above, it soon became clear that these simulations

had not yet converged due to relatively low mesh numbers. According to an empirical formula for structures with long tapers, an appropriate mesh size  $\Delta Z$  to get a physical wake potential, would satisfied the accuracy condition of  $(\Delta Z)^2 \leq \frac{a\phi\sigma_b}{100}$  [13]; with  $\phi$  the taper angle and  $a = \frac{gr}{2}$ , the chamber height. In our case, this condition results in a mesh size of smaller than 10-20  $\mu\text{m}$ . This small mesh size leads to huge number of mesh cells about several billions and increases the simulation time for above several weeks and requires MPI simulation setup with several cluster nodes. Due to lack of such tools convergence study of these simulation are not yet complete. As a compromise, also, the mesh size could be set up to 10  $\mu\text{m}$  only at the taper location and only in the longitudinal direction. Also, a comparison with theoretical analysis and with other simulation tools such as ImpedanceWake2D would be useful.

Furthermore, the details of impedance spectra are different, when a vacuum background and **PEC walls** are used instead of PEC background (Figures 2a and 4. right). Optimizing best simulation conditions and closest simplified model to the reality of such large and complex structure is a challenge and still in progress. Further simulations are also ongoing for IVUE32, regarding geometrical tolerances such as: possible horizontal wiggles of the RF shields (due to non-perfect adjustment of magnet girder position), possible misalignment in the horizontal orientation of the foils, and alternative geometry of slits.

## CONCLUSION AND OUTLOOK

The impedance spectra, and vertical kick factors have been calculated for simplified CPMU17 and IVUE32 models, and the preliminary results have been presented. However, these simulation should be repeated with much higher mesh numbers for a more reliable results. Further simulations could also be done using another model by assuming the vacuum tank and the magnet girders together as a round ridge waveguide [14, 15] as well as heat load computation.

## REFERENCES

- [1] J. Bahrtdt *et al.*, “Characterization and Implementation of the Cryogenic Permanent Magnet Undulator CPMU17 at Bessy II”, in *Proc. 10th Int. Particle Accelerator Conf. (IPAC’19)*, Melbourne, Australia, May 2019, pp. 1415–1418. doi:10.18429/JACoW-IPAC2019-TUPGW014
- [2] M. Huck, J. Bahrtdt, H. Huck, A. Meseck, and M. Ries, “Transverse Broad-band Impedance Studies of the New In-vacuum Cryogenic Undulator at Bessy II Storage Ring”, in *Proc. IBIC’20*, Santos, Brazil, Sep. 2020, pp. 263–267. doi:10.18429/JACoW-IBIC2020-THPP26
- [3] M. Huck, J. Bahrtdt, A. Meseck, G. Rehm, M. Ries, and A. Schaelicke, “Experimental Studies of the In-Vacuum-Cryogenic Undulator Effect on Beam Instabilities at BESSY II”, presented at the IPAC’21, Campinas, Brazil, May 2021, paper WEPAB134, this conference.
- [4] J. Bahrtdt, W. Frentrop, S. Grimmer, C. Kuhn, C. Rethfeldt, M. Scheer, and *et al.*, “In-Vacuum APPLE II Undulator”, in *Proc. IPAC’18*, Vancouver, BC, Canada, Apr. 4., pp. 4114–4116. doi:10.18429/JACoW-IPAC2018-THPMF031
- [5] J. Bahrtdt and S. Grimmer, “In-vacuum APPLE II undulator with force compensation”, *AIP Conference Proceedings*, vol. 2054, p. 030031, 2019. doi:10.1063/1.5084594
- [6] “Computer Simulation Technology (CST), CST Studio Suit, particle dynamics, accelerator components, cavities, wake fields”, <https://www.3ds.com/products-services/simulia/products/cst-studio-suite/solvers/>.
- [7] D. Teytelman, J. Fox, S. Prabhakar, and J. M. Byrd “Characterization of longitudinal impedances in storage rings via multibunch effects”, *Phys. Rev. ST Accel. Beams*, vol. 4, p. 112801, 2001. doi:10.1103/PhysRevSTAB.4.112801
- [8] A. W. Chao, *Physics of collective beam instabilities in high-energy accelerators*. New York, NY, USA: Wiley, 1993.
- [9] Benoit Salvant, “Transverse single-bunch instabilities in the CERN SPS and LHC”, *Beam physics for FAIR Workshop*, Bastenhaus, Germany, Jul. 2010.
- [10] C. Zannini, “Electromagnetic simulation of CERN accelerator components and experimental applications”, Dissertation, Phys. Dept., Ecole Polytechnique Federale de Lausanne, Lausanne, Switzerland, 2013.
- [11] O. A. Tanaka *et al.*, “Impedance evaluation of in-vacuum undulator at KEK Photon Factory”, *J. Phys.: Conf. Ser.*, vol. 1067, p. 062008, 2018. doi:10.1088/1742-6596/1067/6/062008
- [12] B. W. Zotter and S. A. Kheifets, *Impedances and Wakes in High Energy Particle Accelerators*. Singapore:World Scientific, 1998.
- [13] O. Frasciello, S. Tomassini, M. Zobov, A. Grudiev, N. Mounet, and B. Salvant, “Wake fields and impedances of LHC collimators”, *SIF 2014, 100th National Congress*, Sep. 2014.
- [14] K. Tian, J. J. Sebek, A. D. Ringwall, and Z. Li, “Damping trapped modes in an in-vacuum undulator at a synchrotron radiation light source”, *Phys. Rev. Accel. Beams*, vol. 22, p. 050702, 2019. doi:10.1103/PhysRevAccelBeams.22.050702
- [15] K. Tian, J. Sebek, and J. L. Vargas, “Investigation of transverse beam instability induced by an in-vacuum undulator at SPEAR3”, SLAC National Accelerator Laboratory, Menlo Park, USA, Rep. SLAC-PUB-16824.